Numerical Analysis of a Cigar Antenna

Junji Yamauchi, #Hayafumi Harada, and Hisamatsu Nakano
Faculty of Science and Engineering, Hosei University
3-7-2 Kajino-cho, Koganei, Tokyo 184-8584 Japan,
e-mail: hayafumi.harada.u2@stu.hosei.ac.jp

Abstract

A cigar antenna fed by a metallic waveguide is analyzed using the body-of-revolution FDTD method. The effective relative permittivity of the cigar structure is numerically evaluated. The properties of the cigar antenna agree with those of a dielectric rod antenna whose effective permittivity is regarded as being the same.

Keywords : Cigar antenna Dielectric rod antenna Finite-difference time-domain method Effective relative permittivity

1. Introduction

It is well known that a surface wave structure can be employed as a simple antenna with a relatively high gain in the microwave and millimetre-wave regions [1]-[5]. The directivity is characterized by the radiation fields generated at the free and feed ends of the surface wave structure [3]-[5]. Therefore, an appropriate gain can be obtained with a choice of the structure length. A cigar (metallic-disc-on-rod) antenna proposed by Simon *et al.* [6] is one of the promising candidates for this purpose, since it achieves low weight and heat resistance. However, theoretical studies have not been fully carried out until the present time.

The purpose of this paper is to numerically reveal the radiation characteristics of a cigar antenna fed by a metallic waveguide. The body-of-revolution finite-difference time-domain (BOR-FDTD) method [7] is employed for the analysis. We demonstrate that the properties of the cigar antenna are similar to those of the dielectric rod antenna whose effective relative permittivity is chosen to be the same.

2. Configuration and Numerical Method

Figure 1 shows the configuration of a cigar antenna fed by a metallic waveguide (WCI-120) whose inner diameter is $2\rho = 17.475$ mm. The waveguide is excited with the TE_{11} mode at a center frequency of 11 GHz (λ_{11}=27.3 mm). The tapered dielectric rod whose relative permittivity is $\varepsilon_r = 2.05$ is inserted into the metallic waveguide so that the impedance matching may be made between the air-filled and dielectric-filled regions [5].

The effective relative permittivity of the cigar structure depends on a period length Λ, a disk diameter $2\rho_{disk}$ and a boom diameter $2\rho_b$. In this analysis, these parameters are adjusted so as to realize almost the same effective relative permittivity as that observed in the reference dielectric rod antenna shown in Fig. 2. Note that the cigar and dielectric rod antennas are compared under the condition of the same axial length L_{ax}. We treat two types of cigars #1 and #2 with $2\rho_b \approx 0.11\lambda_{11}$. #1 is the model in which the periodicity is chosen to be small, while #2 is the model with a relatively large periodicity. To be specific, the parameters for #1 are $\Lambda = 0.09\lambda_{11}$ and $2\rho_{disk} \approx 0.28\lambda_{11}$, while those for #2 are $\Lambda = 0.27\lambda_{11}$ and $2\rho_{disk} \approx 0.32\lambda_{11}$. It is assumed that the cigar structure is perfectly conducting. To support the cigar, we introduce a short dielectric rod with a diameter of $2\rho_d \approx 0.38\lambda_{11}$ and a length of $L_d = 0.5(\lambda_{11} + \Lambda)$ at the junction between the metallic waveguide and the cigar.

In the analysis, we employ the BOR-FDTD method [6], in which a circular interface is accurately described in the cylindrical-coordinates-based Yee mesh. The partial derivative with

respect to ϕ can be performed analytically, so that the original three-dimensional (r, ϕ, z) model is reduced to an equivalent two-dimensional (r, z) one. This greatly contributes to reduction in the computational time and memory. The calculation parameters are chosen to be $\Delta r = \rho/30 \approx 0.29$ mm and $\Delta z = \lambda_{11}/100 \approx 0.27$ mm. The boundary condition based on the second-order Higdon's operator is placed to absorb outgoing waves at the computational edges.

3. Discussion

Figure 3 shows the gain characteristic at 11 GHz as a function of axial length L_{ax}. The data presented by red solid and open circles show the calculated gains for #1 and #2, respectively, while a black solid circle shows for the reference dielectric rod. In all the results, the gain increases as L_{ax} is increased. As can be seen, the gain property of the cigar is in a good correlation with that of the dielectric rod. It is confirmed that the cigar structure operates as an artificial dielectric. The gain reaches a maximum value of 19.4dBi, when L_{ax} is taken to be around $20\lambda_{11}$. In the following analysis, we typically treat the structures with $L_{ax} \approx 13\lambda_{11}$.

Figure 4 presents the radiation patterns in the E-plane. It is found that similar patterns are observed for all the antennas to be examined. The half-power beamwidths are calculated to be ±7.9 degrees and ±8.1 degrees in the E- and H-planes, respectively. The radiation pattern for circularly polarized wave excitation is illustrated in Fig. 5. In all the results, the cross-polarization component E_L is less than -30 dB around the axial direction.

We now consider the frequency characteristics. The frequency response of the gain is shown in Fig. 6. A gain of more than 17dBi is obtained for #1 over a frequency range of 10.4 to 12.2 GHz. A maximum gain of 18.6dBi is obtained at 11 GHz. It is found that the gain bandwidth for #1 is wider than that for #2, and is close to that observed for the reference dielectric rod. In other words, when the periodicity of the circular disk is sufficiently small compared with the wavelength, the bandwidth becomes almost the same as that for the dielectric rod. The return loss for #1 is more than 15dB over a frequency range of 10.5 to 13 GHz, as shown in Fig. 7.

Figures 8(a) and (b) illustrate the currents I ($= I_r + jI_i$) distributed along the cigar structure at 11 GHz and 13 GHz, respectively. As a matter of convenience, the current values obtained on the wall surfaces of disks are sampled and continuously plotted. It is found that the currents are of travelling wave type, as seen from the phase progression. Its amplitude tends to increase with subsequent generation of a standing wave, as the frequency is increased.

The effective relative permittivity as a function of frequency is shown in Fig. 9. The result for the cigar is estimated by the current distribution illustrated in Fig. 8. On the other hand, that for the dielectric rod is calculated from the eigenmode solver using the Yee-mesh-based imaginary-distance beam-propagation method [8]. Good agreement is found to exist between the results for #1 and for the dielectric rod. It should be noted that the values for #2 rapidly deviate from those of the dielectric rod as the frequency is increased. This results in the deterioration of the radiation pattern with an increase in frequency. It can be said that the choice of a sufficiently short period length is extremely important for the wideband properties.

4. Conclusions

The BOR-FDTD method has been employed to investigate the radiation characteristics of the cigar antenna fed by a metallic waveguide. The configuration parameters of the cigar are adjusted so as to realize almost the same effective relative permittivity as that of a dielectric rod. It is found that the gain bandwidth of the cigar approaches that of the dielectric rod with light weight being achieved.

References

[1] T. Takano and Y. Yamada. "The relation between the structure and the characteristics of a dielectric focused horn," *Trans*. *IEICE*, vol. J60-B, no. 8, pp. 593-595, Aug. 1977.

[2] F. J. Zucker, "Surface-wave antennas," in Antenna Engineering Handbook, 4th ed., New York: McGraw Hill, 2007, ch. 10.
[3] T. Ando, J. Yamauchi, and H. Nakano, "Rectangular dielectric-rod fed by metallic waveguide," *Proc. Inst. Elect. Eng. – Microwave Antennas Propagation*, vol. 149, no. 2, pp. 92-97, 2002.
[4] T. Ando, J. Yamauchi, and H. Nakano, "Numerical analysis of a dielectric rod antenna Demonstration of the discontinuity-radiation concept," *IEEE Trans. Antennas Propag.,* vol. 51, no. 8, pp. 2007-2013, Aug. 2003.
[5] T. Ando, I. Ohba, S. Numata, J. Yamauchi, and H. Nakano, "Linearly and curvilinearly tapered cylindrical-dielectric-rod antennas," *IEEE Trans. Antennas Propag.,* vol. 53, no. 9, pp. 2827-2833, Sept. 2005.
[6] J. C. Simon and G. Weill, "A new type of antenna for endfire radiation," *Ann. Radioelectricite*, vol. 8, pp. 183-193, 1953.
[7] A. Taflove and S. Hagness, Computational Electrodynamics: The Finite-Difference Time-Domain Method, 2nd ed., Boston: Artech House, 2000.
[8] T. Ando, H. Nakayama, S. Numata, J. Yamauchi, and H. Nakano, "Eigenmode analysis of an optical waveguide by a Yee-mesh-based imaginary-distance propagation method for an arbitrary dielectric interface," *J. Lightwave Technol.*, vol. 20, no. 8, pp. 1627-1634, 2002.

Acknowledgments

This paper was supported in part by MEXT, Grant-in-Aid for Scientific Research (22560350).

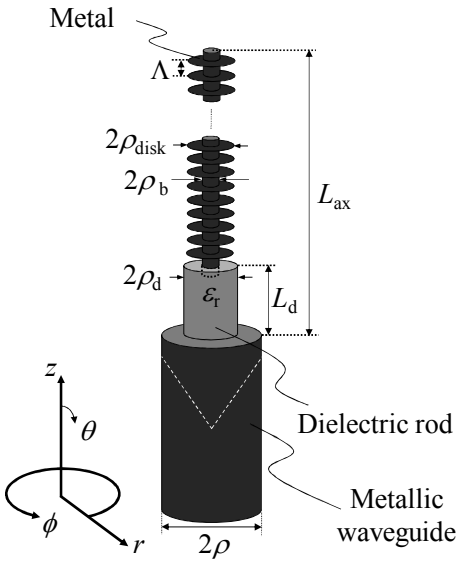

Figure 1: Cigar antenna.

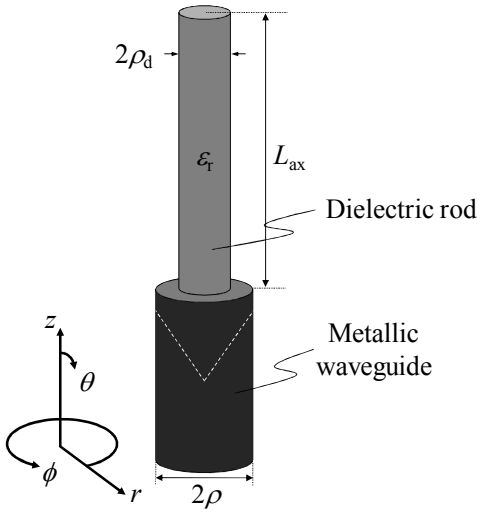

Figure 2: Reference dielectric rod antenna.

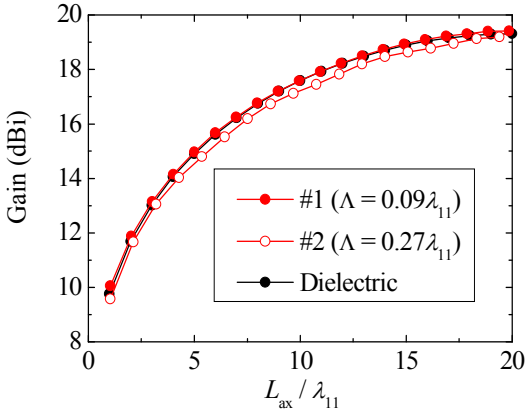

Figure 3: Gain characteristic as a function of L_{ax}.

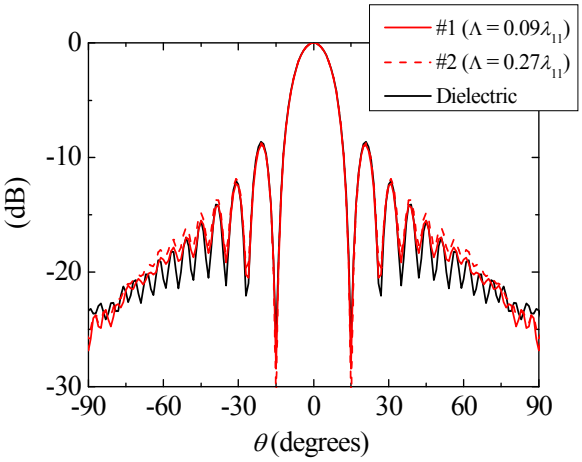

Figure 4: Radiation pattern (E-plane).

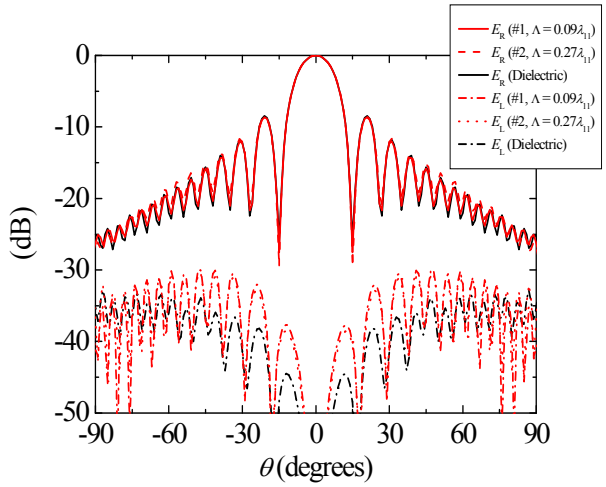

Figure 5: Radiation pattern (circularly polarized wave).

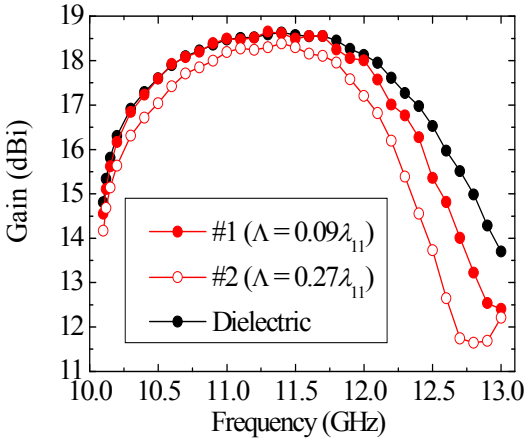

Figure 6: Frequency response of gain.

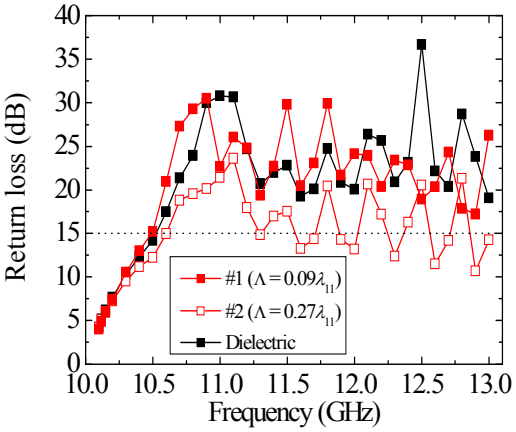

Figure 7: Frequency response of return loss.

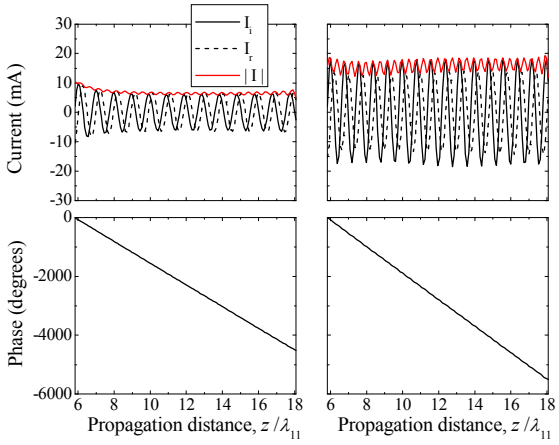

(a) 11GHz (b) 13GHz

Figure 8: Current distribution.

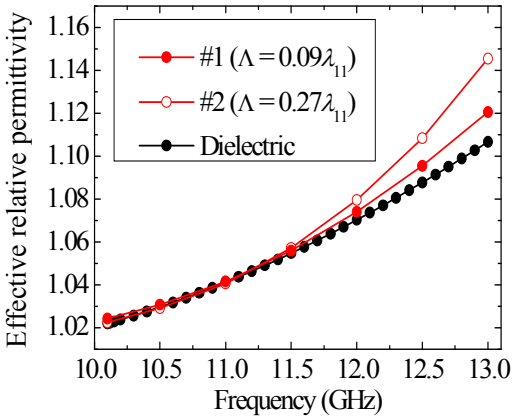

Figure 9: Effective relative permittivity as a function of frequency.